

Dynamic Behavior and Stiffness Tuning in Solenoid Based Ni-Mn-Ga Transducers

LeAnn E. Faidley^a, Marcelo J. Dapino^a, Gregory N. Washington^a, Thomas A. Lograsso^b

^a The Ohio State University, 206 W. 18th Ave, Columbus, OH, USA, 43210

^b Iowa State University, 111A Metals Development, Ames, IA, USA, 50011

ABSTRACT

Ferromagnetic shape memory nickel-manganese-gallium (Ni-Mn-Ga) has shown tremendous promise as an actuator material due to its large strain and high bandwidth. However, current Ni-Mn-Ga devices are electromagnet based as this configuration allows for an externally applied force perpendicular to the applied field, and are therefore bulky, energy inefficient, and narrowband. We investigate the dynamic response of Ni-Mn-Ga driven by a solenoid transducer in which the magnetic field is aligned collinearly with the loading stress. The work focusses on the quasistatic and dynamic testing of a Ni₅₀Mn_{28.7}Ga_{21.3} sample which is believed to have an internal stress field which plays the role of the restoring force necessary for reversible strains. This sample is shown to exhibit reversible compressive strains of -0.41% with no external forces applied. Several experimental apparatus are used in order to verify these results. The measurements demonstrate a 231% change in stiffness with applied dc magnetic fields.

1. INTRODUCTION

In 1996 Ullakko et al¹ reported magnetic-field induced strains of up to 0.2% in stoichiometric Ni₂MnGa at 265 K. As work progressed with this material it was found that certain off stoichiometric compositions can exhibit larger strains of up to 6% at and above room temperature. The large strains and magnetic activation make Ni-Mn-Ga and other Ferromagnetic Shape Memory Alloys (FSMAs) extremely attractive as actuator elements since materials exhibiting both large displacements and fast response times have been rare. These qualities make FSMAs promising for applications such as underwater communications, large structural deformations for morphing unmanned aerial vehicles, and tunable stiffness resonators for noise and vibration control applications. Many of these applications require devices of compact size, high energy density, broad frequency response, and few moving parts which are most easily achievable by solenoid based actuators. However, results in the literature focus primarily on actuators driven by electromagnet which allow for an externally applied orthogonal field-stress pair leading to reversible strain. In this paper, we investigate the response of Ni-Mn-Ga to the collinear field-stress configuration encountered in solenoid based transducers.

Ferromagnetic shape memory refers to either of two mechanisms for magnetic field-induced strain in Ni-Mn-Ga and other FSMAs. One mechanism lies in the structural transformation from austenite to martensite with an applied magnetic field. This transformation is completely reversible upon the removal of the field.² The second mechanism represents the main focus of this work on FSMAs and involves the rearrangement of martensitic twin variants in response to magnetic fields.

Over a certain compositional range the typical martensitic microstructure of Ni-Mn-Ga consists of a mixture of three martensitic variants, each with a tetragonal lattice $a \times a \times c$ ($c < a$), in which adjacent variants are separated by a boundary known as a twin plane.³ The magnetic anisotropy of Ni-Mn-Ga is large in comparison to the energy required to change the volume fraction of each variant; thus the magnetization is rigidly attached to the shorter c-axis.⁴ When a magnetic field is applied, the variants in which the c-axis is aligned with the field

Further author information: (Send correspondence to M.J.D.)

L.E.F.: E-mail: faidley.1@osu.edu, Telephone: 1-614-292-8685

M.J.D.: E-mail: dapino.1@osu.edu, Telephone: 1-614-688-3689

G.N.W.: E-mail: washington.88@osu.edu, Telephone: 1-614-292-8486

T.A.L.: E-mail: lograsso@ameslab.gov, Telephone: 1-515-294-8727

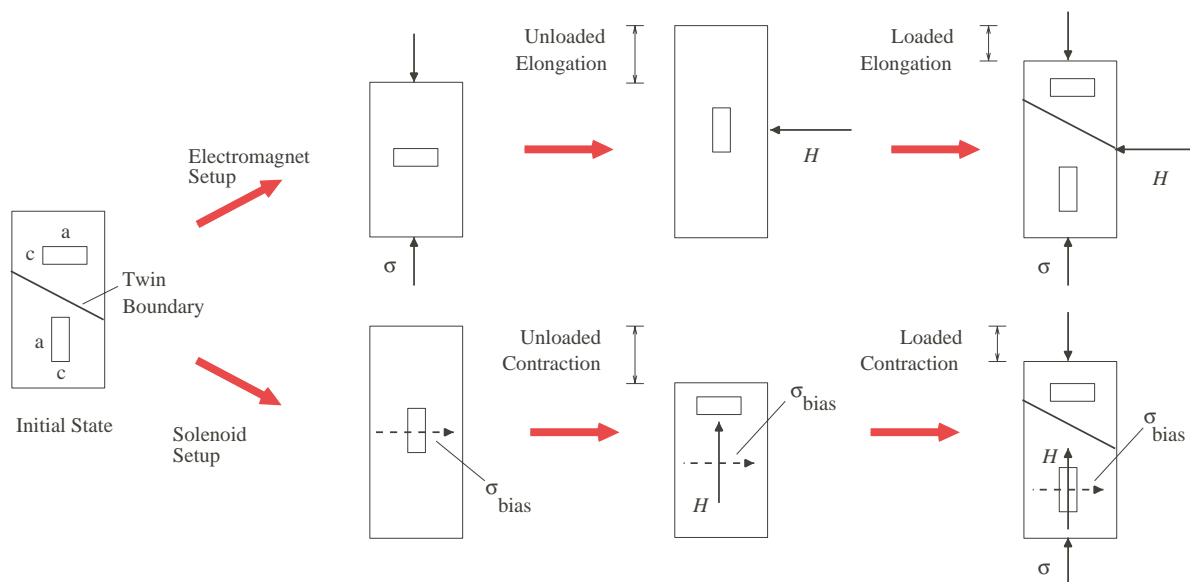


Figure 1. Field-stress orientation for conventional and employed configuration.

are favored, and grow at the expense of the other variants by way of twin boundary motion. Since the c-axis is the shorter of the crystallographic axes, a shortening of the bulk sample in the direction of the field occurs.

In order to achieve the maximum strain from Ni-Mn-Ga, preconditioning, via a magnetic field and mechanical stress, is typically employed to induce a near-single variant with the short c-axis aligned with the axis of the rod. Applying a large magnetic field of approximately 5 kOe orthogonal to the rod axis will induce a near-single variant with the c-axis aligned with the field, creating elongation strains of close to 6% for tetragonal five-layer Ni-Mn-Ga^{5,6} and 9.5% for orthorhombic seven-layer Ni-Mn-Ga.⁷ However, because all twin variants have the same stability, there is no restoring force and the large strain is not recoverable without reconditioning the sample.⁸ In order to achieve reversible strains, a mechanical compressive stress is applied along the rod axis orthogonal to the direction of the magnetic field which favors variants with the c-axis aligned with the stress (see top of Figure 1). Thus, a restoring force is created which leads to reversible strains.⁶

Recent work at The Ohio State University has focused on the use of Ni-Mn-Ga in solenoid based transducers which promise high energy density, compact size, and high frequency response (up to 5 kHz).⁹ In such a configuration the strain is measured along the direction of the applied magnetic field and the applied mechanical loading is parallel to this direction (see bottom of Figure 1). Experimental measurements by Malla et al¹⁰ show that large reversible strains in excess of $-4100 \mu\epsilon$ are achievable in this configuration despite the lack of an externally applied restoring force. It is hypothesized that during the rod manufacture, internal stress concentrations are created orthogonal to the rod axis which play the same role as the externally applied restoring force when the field is applied. One possible source of such internal stress fields are coherent precipitates or retained austenite in the martensite matrix. This would also explain why the collinear stress-field drive configuration can lead to significantly higher material stiffness than previously measured employing conventional electromagnet tests.⁹

This paper focuses on the experimental testing of a $\text{Ni}_{50}\text{Mn}_{28.7}\text{Ga}_{21.3}$ alloy sample in the parallel stress-field configuration. Several different experimental apparatus are used to verify previously presented results indicating large reversible quasistatic strains and large shifts in elastic modulus due to bias magnetic fields. Section 2 will describe these various experimental techniques, the results of which will be presented and discussed in Section 3. The conclusions derived from this study will be summarized in Section 4

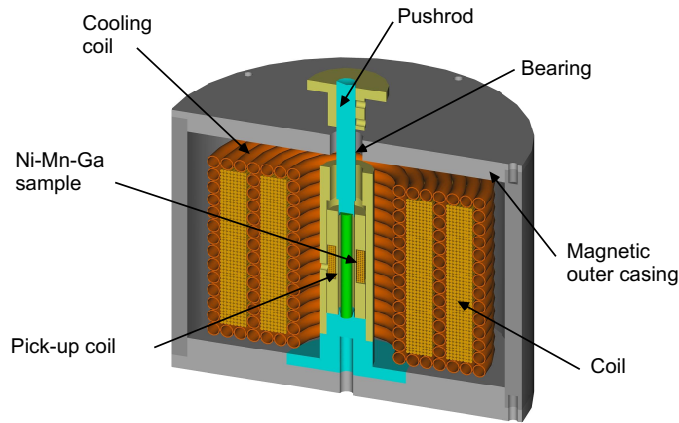


Figure 2. Cross section of the broadband transducer employed in this study.

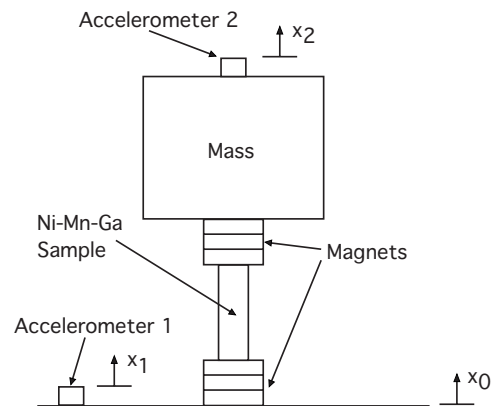


Figure 3. Shaker set-up used for dynamic modulus shift verification.

2. EXPERIMENTS

The experiments are focused on the quasistatic and dynamic characterization of a single crystal alloy with composition $\text{Ni}_{50}\text{Mn}_{28.7}\text{Ga}_{21.3}$ which was prepared by the Bridgman method. The single crystal ingot was oriented along the $[100]$ direction, and a 0.248 in (0.630 cm) diameter, 0.883 in (2.243 cm) long rod was cut from the ingot using electrical discharge machining (EDM).

Several different experimental arrangements are used in the characterization and verification of the sample. The primary apparatus is the collinear magnetic field-stress, broadband research transducer shown in Figure 2, which consists of a water-cooled solenoid, pickup coil, and magnetic steel components integrated to form a closed magnetic circuit. The closed magnetic circuit ensures that demagnetization factors are negligible and magnetic forces exerted on the magnetic pushrod are accounted for in the measurements.

The solenoid consists of 1350 turns of AWG 15 magnet wire and has a field rating of 167 Gauss/A, up to 8.1 kGauss. Distributed within the solenoid lies a coil of 0.25 in diameter copper tubing which provides temperature control within $\pm 1^\circ\text{F}$ by means of water flow at a rate of up to 6.35 L/min. The solenoid is driven by two 4 kW Techron amplifiers arranged in series, with an overall voltage gain of 60 and a maximum output current of 56 A at the nominal solenoid resistance of $3.7\ \Omega$. The magnetic induction is measured with a pickup coil made from AWG 33 insulated copper wire wound in two layers around an aluminum spool. Several Omega thermocouples are used to monitor the system temperature through a 10-channel Omega signal conditioner. The system is controlled by a SigLab 20-42 data acquisition system interfaced through a PC. The test setup is illustrated in Figure 4.

The research transducer shown in Figure 2 and its individual components are used in various arrangements for the collection of the data discussed in this paper. The broadband transducer is used in its entirety to run dynamic tests in which the resonance of the rod is found using swept sine excitation between 100 and 5000 Hz. PCB accelerometers U352C22 and 352C68 are used to measure the acceleration of the pushrod and canister while masses of various sizes are loaded on the pushrod.

The solenoid and outer casing of the broadband transducer are employed without the rest of the central components in the measurement of the quasistatic strains. In these tests the transducer is turned horizontally and a strain-gaged sample is securely mounted on a non-magnetic support structure in its center such that the sample is in an unloaded state. Fields of up to 700 kA/m are then applied at a frequency of 0.1 Hz. These tests are designed to closely mimic the conditions a sample is exposed to in an electromagnet and to eliminate uncertainties in the data collection due to the behavior of the steel components of the transducer in the large magnetic fields. For verification of this quasistatic strain data the Ni-Mn-Ga sample was also tested by the

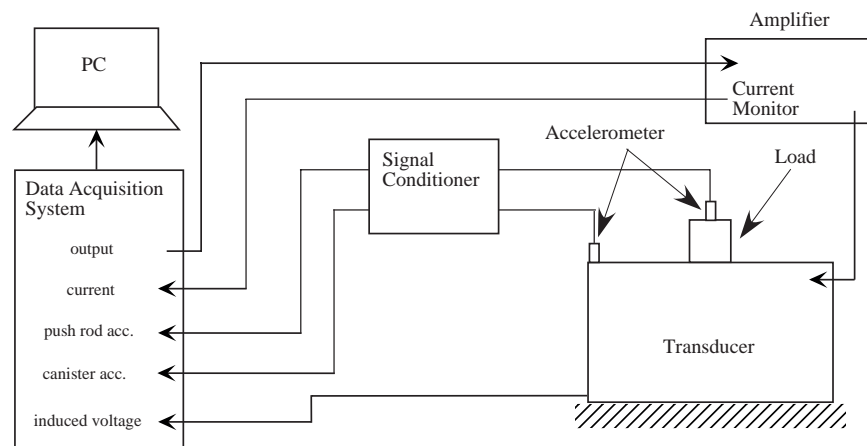


Figure 4. Experimental setup used for dynamic testing of Ni-Mn-Ga.

Magnetics Group of the Department of Energy's Ames Laboratory and the Magnetic Materials Group at the Naval Surface Warfare Center.

The secondary apparatus shown in Figure 3 is used to verify the dynamic data of the Ni-Mn-Ga sample in isolation from the complexity of the transducer assembly. In this arrangement the sample is mounted to the top of a Labworks ET-126 shaker driven by a Labworks PA-138 amplifier. The sample is mounted in series with different combinations of Nd-Fe-B permanent magnets in order to create bias magnetic fields of between 6.24 and 379.2 kA/m. Loads ranging from 0 to 250g are mounted on top of the sample. The outputs from the system are the accelerations of the platform (\ddot{x}_1) and the load (\ddot{x}_2) which are measured using PCB U353B16 and PCB U352C22 accelerometers, respectively. The input is the displacement of the platform (x_0) which is controlled according to a swept-sine excitation from 100 to 10000 kHz provided by the data acquisition system (SigLab 20-42). The transfer function between the load and platform accelerations is recorded for purposes of determining the resonance frequency and then calculating the elastic modulus of the rod.

3. DISCUSSION OF RESULTS

3.1. Quasistatic Testing

Our results from the quasistatic strain testing of the $\text{Ni}_{50}\text{Mn}_{28.7}\text{Ga}_{21.3}$ sample have been presented by Malla.¹⁰ The study presented here eliminates the effects of the steel components in the magnetic circuit by removing the central part of the transducer. The sample is placed on a non-magnetic mount which is inserted into the solenoid such that the rod lies horizontally along the axis of the coil in an unloaded configuration. Using this arrangement, Figure 5 shows the results when an ac field of 700 kA/m and 0.1 Hz is applied to the sample. The strain is measured using strain-gages mounted to both sides of the sample. A maximum compressive strain of $3970 \mu\epsilon$ was measured of which $3840 \mu\epsilon$ is reversible. This strain, though smaller than the maximum reported for Ni-Mn-Ga in the conventional orthogonal stress-field orientation, still represents a 2.5x improvement over the reversible strain achievable by the technologically mature magnetostrictive material Terfenol-D ($1600 \mu\epsilon$)¹¹ used in a similar solenoid based transducer.

Figure 6 shows results for quasistatic tests run in fields generated by an electromagnet at the DoE's Ames Laboratory.¹² For this test the $\text{Ni}_{50}\text{Mn}_{28.7}\text{Ga}_{21.3}$ sample was strain-gaged and mounted at the center of the electromagnet such that the field was applied along the rod axis. The field was then slowly cycled up to a maximum of 600 kA/m and down to a minimum of -600 kA/m. The results show the same negative strains and hysteresis as the solenoid tests in Figure 5. The magnitude of the strain generated in the electromagnet is about $4200 \mu\epsilon$, which varies from the solenoid-produced strains by only 5% due to differences in strain-gage attachment and sample mounting techniques. In addition, tests conducted in an electromagnet at the Naval Surface Warfare

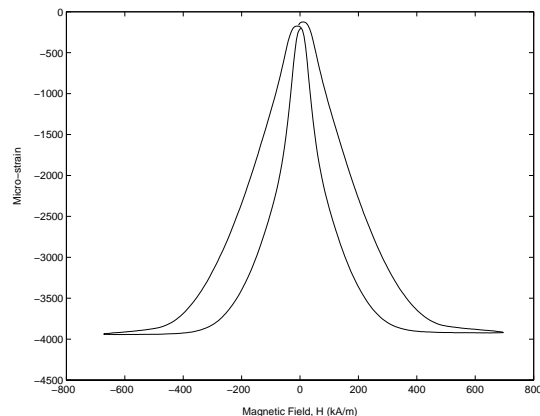


Figure 5. Quasistatic strain response for Ni-Mn-Ga in solenoid produced field (axial field configuration).

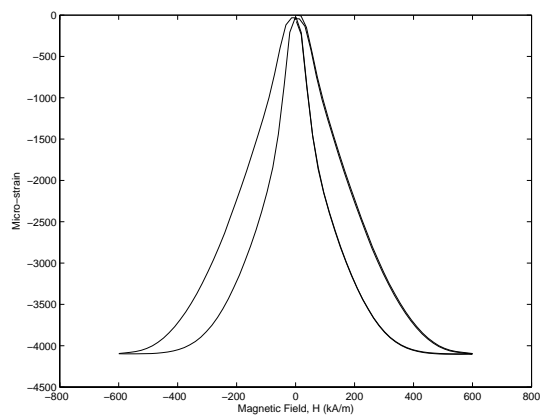


Figure 6. Quasistatic strain response for Ni-Mn-Ga in electro-magnet produced field (axial field configuration).

Center¹³ also confirmed contraction strains of 4000 $\mu\epsilon$ in tests in which the length of the rod was measured after the application of a 7 kOe field in directions parallel and orthogonal to the rod axis.

These three sets of tests verify the capability for Ni-Mn-Ga to produce reversible strain in the parallel stress-field configuration despite the lack of an external orthogonal restoring force. As mentioned previously, existing models for this material proposed by both Likhachev¹⁴ and O'Handley¹⁵ indicate that such a force is necessary in order to revert the sample to its original shape after the application of the magnetic field. This may suggest the existence of an *internal* restoring force in this sample which may be caused by the presence of impurities or retained austenite precipitates which create a stress field in the martensite matrix.

3.2. Dynamic Elastic Modulus Testing

Two different methods are used to dynamically determine the shift in the elastic modulus of $\text{Ni}_{50}\text{Mn}_{28.7}\text{Ga}_{21.3}$ due to a bias magnetic field. In the first,⁹ the sample is excited magnetically using the transducer in Figure 2 and the system resonances are determined from the transfer function relating the acceleration of the pushrod to the input voltage to the system. Various methods, including varying core materials and loads, are used to determine which of the peaks in this transfer function are most closely related to the stiffness of the sample. Various bias magnetic fields between 0 and 130 kA/m are then applied and swept-sine excitation tests are run from 100 to 5000 Hz. The results of these tests for a load of 250g are shown in Figure 7. The increase in resonance frequency as bias field is increased is an indication of the stiffening of the sample. This shift in elastic modulus can be quantified through the use of a simple 1 degree of freedom model and a linear model for rod vibration. The equations,

$$(2\pi f)^2 = \frac{k}{m} \quad (1)$$

$$k = \frac{AE}{l}, \quad (2)$$

where f is the resonance frequency in Hz, k is the stiffness of the rod, m is the mass of the load plus the effective dynamic mass of the rod ($\frac{1}{3}$ the mass of the rod), A is the cross-sectional area of the rod, l is the length of the rod, and E is the elastic modulus can then be used to determine values for the elastic modulus and its change. The calculated values for change in elastic modulus relative to the zero field case are shown for different field levels in the top part of Figure 7(b). The bottom part of this figure shows the relationship between the heights of the resonance peaks in Figure 7(b) (shown as points) and the line representing $C\sqrt{km}$ where C is an appropriately chosen constant. This indicates the agreement between the collected data and the second order model for damping which states that the peak height is inversely proportional to the damping which is inversely

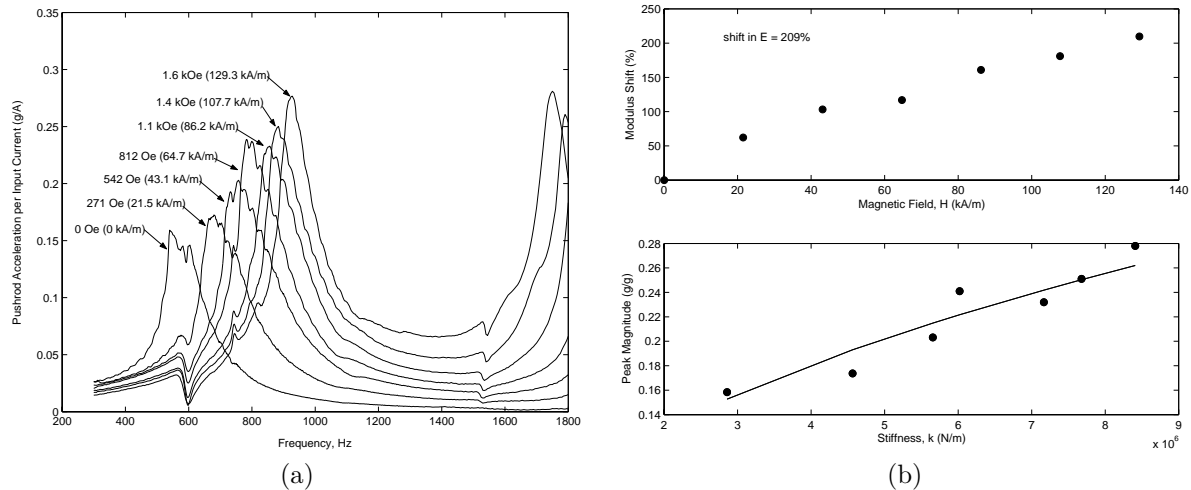
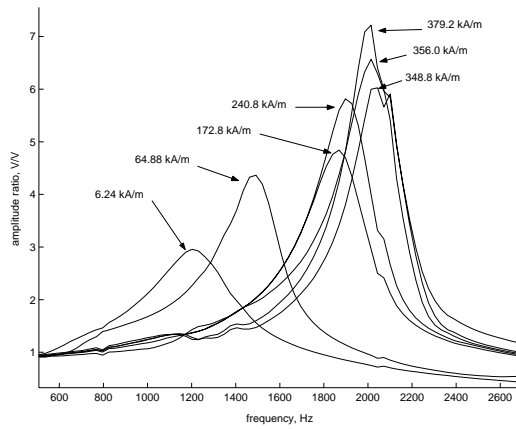


Figure 7. Dynamic magnetic excitation of Ni-Mn-Ga for various applied fields and 250 gram load.

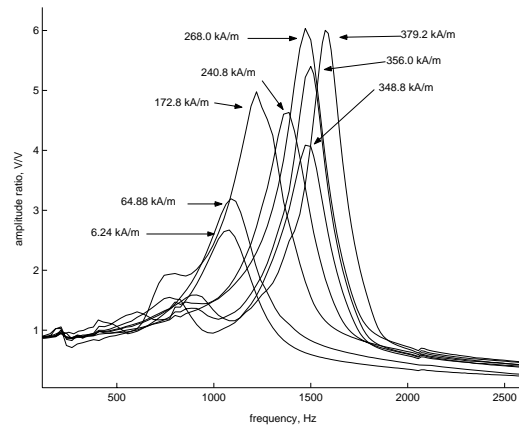
proportional to \sqrt{km} . As can be seen, for the 250g case the shift in elastic modulus relative to the minimum is monotonically increasing with a magnitude of 209% with a 1.6 kOe shift in field. This is on the order of the shift seen in magnetostrictive Terfenol-D of about 200%.¹⁶ Other tests run in this earlier study⁹ suggest a dependence of the magnitude of the modulus shift on applied load as evidenced by the 83% shift seen for a 60g load.

The complexity of the broadband transducer and the possible effects of large magnetic fields on many of its components create difficulties in determining how much of the shift in elastic modulus measured in these tests is a result of the Ni-Mn-Ga sample itself. In order to alleviate these problems and verify this effect, the Ni-Mn-Ga sample was isolated from the transducer using the experimental configuration shown in Figure 3. For these tests, the sample was excited mechanically using a swept-sine input to a shaker. The bias magnetic field was provided by various combinations of Nd-Fe-B permanent magnets which were inserted in series with the sample. Transfer functions between the rod's base acceleration and the acceleration of the load on top of the rod were collected for the frequency range of 100 to 10000 Hz, as shown for the 50 and 100 gram cases in Figure 8. It is noted that due to the experimental set up it was impossible to increase the magnetic field through the sample without also increasing the load on the sample. This obscures any clear trend in resonance location or peak height that would be apparent through the raw data in Figure 8. Using Equations (1) and (2) however, the elastic modulus of the sample can be calculated taking into account the increase in load due to the addition of magnets on the top of the rod. The shift in elastic modulus relative to its value at zero field is then calculated and is plotted in Figure 9 for various loads. The lower part of the individual plots in this figure show the heights of resonance peaks as compared to the expected trend due to the dependence of damping on $C\sqrt{km}$.

The data in Figure 9 verify the existence of a stiffening effect of the $\text{Ni}_{50}\text{Mn}_{28.7}\text{Ga}_{21.3}$ sample in response to applied bias magnetic fields. The maximum shift in elastic modulus measured was 231% which is on the order of the 209% measured dynamically in the transducer and the 186% measured statically by Malla.¹⁷ Figure 9 also confirms the suggestion generated by previous data that there is an optimal load which will allow for the maximum shift in elastic modulus for a given change in field. From this data it would seem that this optimal load is between 20 and 100g since the 50g load exhibits a shift of 231% while the 100g load shows a 137% shift and the shifts for both the 20 and 250 g loads are significantly smaller. The data presented in the bottom part of the plots in Figure 9 show that the expected trend is seen in the resonance peak height, indicating that the damping of the Ni-Mn-Ga is not dependent on the bias field. There is some variation from the trend especially in the 100g case which may be caused by the high sensitivity of the peak height to changes in damping due to the connections between magnets, the load, and the sample.

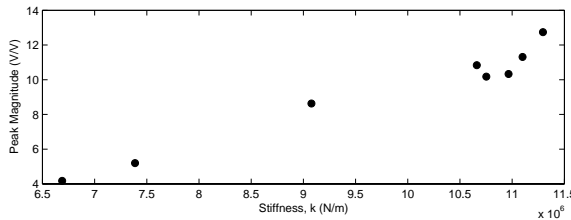
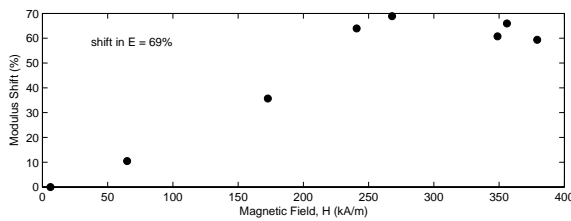


(a) 50 gram load

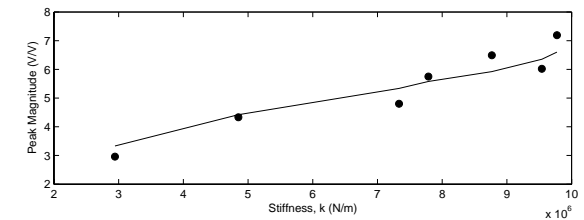
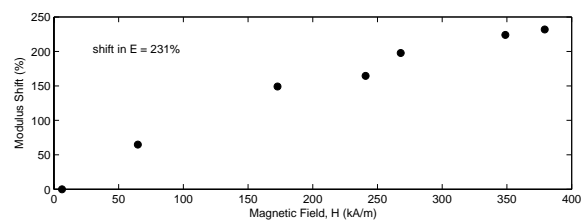


(b) 100 gram load

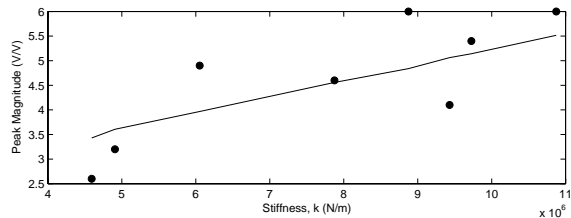
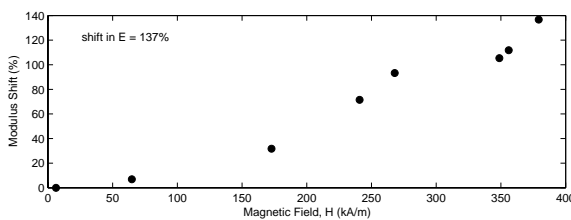
Figure 8. Dynamic mechanical excitation of Ni-Mn-Ga for various applied fields and loads.



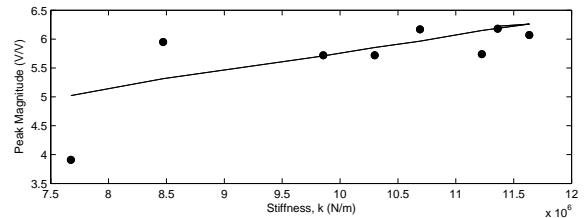
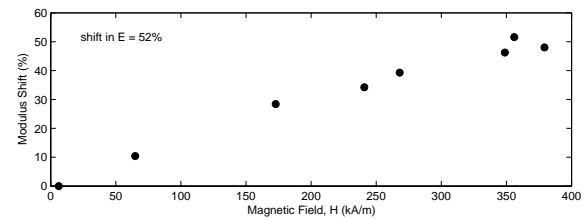
(a) 20 gram load



(b) 50 gram load



(c) 100 gram load



(d) 250 gram load

Figure 9. Calculated elastic modulus shift and damping trend for various loads.

4. CONCLUSIONS AND FUTURE WORK

This paper has presented quasistatic and dynamic characterization of a $\text{Ni}_{50}\text{Mn}_{28.7}\text{Ga}_{21.3}$ cylindrical sample when exposed to an axial magnetic field. Compressive quasistatic strains of $-4100\ \mu\epsilon$ under fields of 600 kA/m have been measured in a solenoid and two independently run electromagnet tests. The fact that this strain is reversible despite the lack of an externally applied orthogonal restoring force suggests the existence of an internal stress field created during the sample's manufacture. In addition, a shift in elastic modulus of up to 231% with bias magnetic field has been verified using dynamic tests with both magnetic and mechanical excitations for the sample in the solenoid transducer and independent from it.

The confirmation of both the quasistatic strain and the modulus shift indicates that Ni-Mn-Ga is a promising core material for solenoid transducers. Future work in this area will investigate the sources of the internal stresses which allow reversible strains under coaxial applied fields so that such samples can be more easily manufactured and the output strains may be increased. Models will be developed to describe the highly nonlinear behavior of this material and then control strategies will be created that make use of this model in order to control applications of Ni-Mn-Ga based solenoid transducers.

5. ACKNOWLEDGMENTS

The authors would like to acknowledge Mr. Aayush Malla for his aid in some of the experimental testing, D.C. Jiles et al. at the Department of Energy, Ames Lab, and A.E. Clark et al. at the Naval Surface Warfare Center for their help in the electromagnet verification testing of the Ni-Mn-Ga sample. In addition L.E.F. would like to recognize the Ohio Space Grant Consortium for funding her work.

REFERENCES

1. K. Ullakko, J. Huang, C. Kantner, R. O'Handley, and V. Kokorin, "Large magnetic-field-induced strains in Ni_2MnGa single crystals," *Appl. Phys. Lett.* **69**, pp. 1966–1968, September 1996.
2. R. James and M. Wuttig, "Magnetostriiction of martensite," *Philosophical Magazine A* **77**(5), pp. 1273–1299, 1998.
3. R. Tickle, R. James, T. Sheild, M. Wuttig, and V. Kokorin, "Ferromagnetic shape memory in the NiMnGa system," *IEEE Trans. Magn* **35**, pp. 4301–4310, 1999.
4. K. Ullakko, "Magnetically controlled shape memory alloys: A new class of actualtor materials," *Journal of Materials Engineering and Performance* **5**, pp. 405–409, June 1996.
5. S. Murray, M. Marioni, P. Tello, S. Allen, and R. O'Handley, "Giant magnetic-field-induced strain in $\text{Ni} - \text{Mn} - \text{Ga}$ crystals: experimental results and modeling," *Journal of Magnetism and Magnetic Materials* **226-230**, pp. 945–947, May 2001.
6. A. Likhachev, A. Sozinov, and K. Ullakko, "Influence of external stress on the reversibility of magnetic-field-controlled shape memory effect in Ni-Mn-Ga," *Proceedings of SPIE Smart Structures and Materials Conf.* **4333**, pp. 197–206, 2001.
7. A. Sozinov, A. Likhachev, N. Lanska, and K. Ullakko, "Giant magnetic-field-induced strain in NiMnGa seven-layered martensitic phase," *Applied Physics Letters* **80**, pp. 1746–1748, March 2002.
8. S. Murray, M. Marioni, S. Allen, R. O'Handley, and T. Lograsso, "6% magnetic-field-induced strain by twin-boundary motion in ferromagnetic Ni-Mn-Ga," *Applied Physics Letters* **77**(6), pp. 886–888, 2000.
9. L. E. Faidley, M. J. Dapino, G. N. Washington, and T. A. Lograsso, "Dynamic response in the low-khz range and delta-e effect in ferromagnetic shape memory $\text{Ni} - \text{Mn} - \text{Ga}$," *Proceedings of IMECE 2003* (43198), Forthcoming.
10. A. Malla, M. Dapino, and T. Lograsso, "Effect of composition on the magnetic and elastic properties of shape memory NiMnGa ," *Proceedings of SPIE Smart Structures and Materials Conf.*, March 2003.
11. M. J. Dapino, A. B. Flatau, and F. T. Calkins, "Statistical analysis of Terfenol-D material properties," *Proceedings of SPIE Smart Structures and Materials Conf.* **3041**(20), 1997.
12. J. Paulsen, "Private Correspondence from DoE - Ames Lab - Magnetism Focus." August 2003.
13. J. Restorff, "Private Correspondence from Navel Surface Warfare Center - Magnetic Materials Group." December 2003.

14. A. Likhachev and K. Ullakko, "The model of magnetic-field-controlled shape memory effect in *NiMnGa*," *J. Phys. IV France* **11**(Pr8), pp. 293–298, 2001.
15. R. C. O'Handley, "Model for strain and magnetization in magnetic shape-memory alloys," *Journal of Applied Physics* **83**, pp. 3263–3270, March 1998.
16. A. B. Flatau, M. J. Dapino, and F. T. Calkins, "High bandwidth tunability in a smart vibration absorber," *J. Intell. Mater. Syst. and Struct.* **11**, pp. 923–929, Dec 2000.
17. A. Malla, "Effect of composition of the magnetic and elastic properties of shape memory Ni – Mn – Ga," Master's thesis, The Ohio State University, June 2003.